International Journal of Thermofluid Science and Technology (2022)
Volume 9, Issue 5, Paper No. 090504
https://doi.org/10.36963/IJTST.2022090504
Research Article

Onset of surface driven convection in selfrewetting fluid layer overlying a porous medium

Gangadharaiah Y H

Department of Mathematics, RV Institute of Technology and Management, Bangalore, India

ARTICLE INFO

Received: 16 Aug. 2022;
Received in revised form:
16 Oct. 2022;
Accepted: 01 Nov. 2022;
Published online:
08 Nov. 2022

Keywords:
bilinear system
Self-rewetting
Surface tension.

ABSTRACT

The onset of thermocapillary convective motion in a self-rewetting fluid layer overlying a porous medium with thermally dependent surface tension is studied analytically. Surface tension is assumed to be a quadratic function of temperature. The top surface of a fluid layer is deformably free and the bottom is rigid. We considered boundaries to be insulating to temperature perturbations. The governing equation that satisfies the composite system is analyzed by the normal mode approach and solved by the regular perturbation technique for linear stability. A mathematical expression is derived for the critical Marangoni number by solving coupled equations. The influence of crispation number, thermal diffusivity ratio, and other physical parameters involved therein are analyzed for the convective stability of the bilayer system. It has been found that the start of convection is delayed when the crispation number goes down and the thermal diffusivity ratio goes up. Also, the impact of the ratio of the thickness of the fluid to the thickness of the porous matrix and the other physical parameters on controlling the convective motion of the configuration is examined in detail.

*Corresponding e-mail: gangu.honnappa@gmail.com (Gangadharaiah Y H)

Nomenclature

a	horizontal wavenumber	M_c	critical Marangoni number
D	differential operator d/dz	Da	Darcy number
ρ_0	fluid density	p	pressure
σ	surface-tension	ϕ	porosity
W	perturbed vertical velocity	T	temperature
χ	thermal diffusivity ratio	μ	fluid viscosity
β	slip parameter	$\vec{V}$	velocity vector (u, v, w)
∇_h^2	horizontal Laplacian operator	c	specific heat capacity
∇^2	Laplacian operator	B_0	Bond number
Cr	Crispation number	K	permeability
h	depth ratio	θ	amplitude of perturbed temperature

1. Introduction

Thermal gradients cause surface stresses on the free surfaces of fluid flows, which move the bulk phase. The Marangoni effect, also known as thermocapillary, refers to the behavioral motions caused by temperature-dependent surface tension. Temperature variations are used to control the outcome in a variety of situations, such as climbing films, droplet migration, and convection in closed cavities. Benard [1] was the first to conduct mathematical experiments and identify a pattern of cellular convective instability. Pearson [2] explained that surface-tension stresses were more important at the experimental layer heights, even though buoyancy can drive convection in this setup. It has a short (finite) wavelength and doesn't change the shape of the surface much. Nield [3] combined surface tension and buoyancy effects and discovered that they reinforce and are tightly coupled. Li et al. [4] investigate a layer of finite extent and predict multicellular flow structure. The thermocapillary movement of droplets has been examined in various studies in recent years [5-13].

Nield [14] pioneered the research of the instability of a fluid-porous bilayer system. The initiation of convection in a fluid layer overlaying a porous medium layer was explored in this research, with the upper surface considered to be deformable. Chen and Chen [15, 16] investigated the start of finger convection in a similar system with a non-deformable free surface using linear stability analysis and experiments. Darcy's law and the Beavers-Joseph condition [17] are used in their research. It was discovered that the system's instability is bimodal and responds significantly to changes in the depth ratio h. In a similar model, Zhao et al. [18] explored heat effects on Rayleigh-B'enard-Marangoni instability, pointing out that complex phenomena had previously been neglected. They discovered that heat transfer at the free surface can result in a mode transition of convection, which occurs only in a configuration with a strong surface tension effect. A comparable approach is being researched further [19- 28].

Nonlinearity in the connection between surface tension and temperature may be seen in fluids such as aqueous solutions of higher alcohols [29, 30], which differ from the fluids in the publications cited above. Cloot and

Lebon [31] looked at the instability of a fluid with nonlinear temperature-dependent surface tension and proposed a second-order Marangoni number. The inaccuracy produced by neglecting the nonlinear term is also explored in their research. In contrast to ordinary fluids, the surface tension of self-rewetting fluids exhibits a positive gradient beyond a certain temperature value. The experimental results indicate that the use of self-rewetting fluids as working fluid significantly improves the performance of the capillary evaporator by decreasing the casing temperature.

In this article, the thermocapillary convective motion in a porous medium layer below a self-rewetting fluid with a deformable top surface by the regular perturbation method was studied. The influence of crispation number, thermal diffusivity ratio, depth ratio, and the other physical parameters is studied, respectively.

2. Conceptual Model

The bilayer system, of which the sketch is shown in Fig. 1, comprises a layer of self-rewetting fluid and a layer of porous medium saturated with the same fluid. The system is considered two-dimensional and infinite in the horizontal direction x. A uniform vertical temperature gradient $\frac{\partial T}{\partial t} = -b$ (b>0) is imposed on the system. The surface-tension σ exerted at the upper surface is considered to be quadratically dependent on the temperature:

$$\sigma = \sigma_m + \gamma\left(T - T_m\right)^2$$

in which, σ_m represents the minimum surface tension at temperature T_m and γ is a positive parameter.

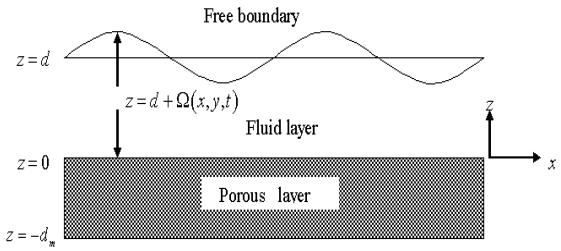

Fig. 1 Physical configuration.

3. Mathematical Formulation

For the proposed scheme, the governing equations are:

Region1: For the fluid layer $\left(0 \le z \le d\right)$

Conservation of mass:

$$\nabla \cdot \vec{V} = 0 \tag{1}$$

Conservation of linear momentum:

$$\frac{D\vec{V}}{Dt} = -\frac{1}{\rho_0}\nabla p + \mu \nabla^2 \vec{V} \tag{2}$$

Conservation of energy:

$$\frac{DT}{Dt} = \kappa \nabla^2 T \tag{3}$$

Region2: For the porous layer ($-d_m \le z \le 0$)

Conservation of mass:

$$\nabla \cdot \vec{V}_m = 0 \tag{4}$$

Conservation of linear momentum:

$$\frac{1}{\phi}\frac{\partial \vec{V}_m}{\partial t} = -\frac{1}{\rho_0}\nabla p_m - \frac{\mu}{K}\vec{V}_m \tag{5}$$

Conservation of energy:

$$\left(\rho c\right)_m \frac{\partial T_m}{\partial t} + \left(\rho_0 c_l\right)\left(\vec{V}_m \cdot \nabla_m\right)T_m = \kappa_m\left(\rho_0 c_l\right)\nabla^2 T_m \tag{6}$$

In these equations above, the subscripts represent the porous layer. ϕ denotes the porosity of the porous layer, K the permeability, and c the specific heat capacity. We scale the coordinate, velocity v, pressure p, temperature difference T-T_0, and time t by d, κ / d , $\rho_0 \kappa \gamma / d^2$, $\Delta T = b\left(d + d_m\right)$, d^2 / γ , respectively.

Perturbations of velocities, pressure, and temperature are introduced and the equations are linearized thereafter. In order to analyze arbitrary disturbance in terms of normal modes, we suppose that the perturbations w and θ have the forms

$$\left(w, \theta\right) = \left[W\left(z\right), \Theta\left(z\right)\right]\exp\left[i\left(lx + my\right)\right] \tag{7}$$

$$\left(w_m, \theta_m\right) = \left[W_m\left(z\right), \Theta_m\left(z\right)\right]\exp\left[i\left(\tilde{l}x + \tilde{m}y\right)\right] \tag{8}$$

The ordinary differential equations,

In region-1,

$$\left(D^2 - a^2\right)^4 W = 0 \tag{9}$$

$$\left(D^2 - a^2\right)\Theta = \frac{-1}{\left(1 + \chi h\right)}W \tag{10}$$

In region-2,

$$\left(D^2 - a^2\right)W_m = 0 \tag{11}$$

$$\left(D^2 - a^2\right)\Theta_m = \frac{-\chi^2}{\left(1 + \chi h\right)}W_m \tag{12}$$

4. Boundary Conditions

On the upper surface z =1, deformable and insulated to temperature perturbation.

$$W = D\Theta = D^2W + M\ a^2\left(\Theta - Z\right) = 0 \tag{13}$$

$$-Cr\left(D^2 - 3a^2\right)DW + \left(B_0 + a^2\right)a^2 Z = 0 \tag{14}$$

At the fluid-porous interface z =0, normal velocity, temperature, heat flux, and normal momentum are assumed continuous and Beaver-Joseph condition [32] is applied.

$$W = W_m \tag{15}$$

$$\Theta = \Theta_m \tag{16}$$

$$D\Theta = \frac{1}{\chi} D\Theta_m \tag{17}$$

$$\left[D^2 - 3a^2\right]DW = \frac{-1}{Da^2h^2} D_m W_m \tag{18}$$

$$\left[D^2 - \frac{\beta}{Da\,h} D\right]W = \frac{-\beta}{Da\,h} D_m W_m \tag{19}$$

On the lower surface, z_m = -h = d/d_m, the boundary is considered to be rigid and insulated to temperature perturbation.

$$W_m = D\Theta_m = 0 \tag{20}$$

In the equations above, the dimensionless parameters are listed:

$$Da = \frac{\sqrt{K}}{d_m}, M = \frac{\gamma\left(\Delta T\right)^2 d}{\left(\mu\kappa\right)}, \chi = \frac{\kappa}{\kappa_m}$$

where Da, M, χ are Darcy number, Marangoni number, and the thermal diffusivity ratio respectively. From these equations and boundary conditions, an eigenvalue problem is formulated, which is solved with the regular perturbation method.

5. Method of Solution

For the steady temperature and concentration flux bounds, convection occurs at a minimum value of a. That is,

$$\left(W, W_m, \Theta, \Theta_m\right) = \sum_{i=0}^{N}\left(a^2\right)^i \left(W_i, W_{mi}, \Theta_i, \Theta_{mi}\right) \tag{21}$$

Substitution of Eq. (21) into Eqs. (9) – (12) and the boundary conditions (13) – (19) and considering like powers of a^2, we get zeroth-order equations whose solutions are as follows

$$W_0 = 0, \quad \Theta_0 = 1 \tag{22}$$

$$W_{m0} = 0, \quad \Theta_{m0} = 1 \tag{23}$$

The equations at the first order in a^2 are For region-1,

$$D^4 W_1 = 0 \tag{24}$$

$$D^2\Theta_1 = -\frac{1}{\left(1+\chi h\right)} W_1 + 1 \tag{25}$$

For region-2,

$$D^2 W_{m1} = 0 \tag{26}$$

$$D^2\Theta_{m1} = W_{m1} + 1 \tag{27}$$

and the boundary conditions(13) –(19) become

$$W_1 = 0,\ D\Theta_1 = 0,\quad D\Omega_1 = 0\ at\quad z = 1 \tag{28}$$

$$D^2 W_1 + M\left(1 - \frac{Cr}{B_0} D^3 W_1\right) = 0\, at\, z = 1 \tag{29}$$

$$W_{m1} = 0, D_m\Theta_{m1} = 0\ at\quad z_m = -h \tag{30}$$

And at the interface

$$W_1 = W_{m1} \tag{31}$$

$$\Theta_1 = \Theta_{m1} \tag{32}$$

$$D\Theta_1 = \frac{1}{\chi} D\Theta_{m1} \tag{33}$$

$$D^3 W_1 = \frac{-1}{h^2 Da^2} DW_{m1} \tag{34}$$

$$D^2 W_1 - \frac{\beta}{h\,Da} DW_1 = \frac{-\beta}{h^2 Da^2} DW_{m1} \tag{35}$$

The general solutions of Eq. (24) and (26) are respectively given by

$$W_1 = \left[C_1 + C_2 z + C_3 z^2 + C_4 z^3\right] \tag{36}$$

$$W_{m1} = \left[C_5 + C_6 z_m\right] \tag{37}$$

where

$$C_1 = \frac{24\left(B_0\chi Da^2 + 48B_0h^2M + \beta\right)}{48B_0Dah - 2Cr\,Dah + M + 10\beta + 48B_0Da^2}$$

$$C_2 = \frac{\left(48B_0h^2Da + M\beta\right)}{48B_0h^2 - 2Cr\,Dah}, C_3 = \frac{\left(\beta\chi Da + 48h^2M\right)}{24B_0 + 24B_0Da^2}$$

$$C_4 = \frac{\left(48B_0h^2\chi M + Da\beta\right)}{48B_0 - B_0\chi Da^2}, C_5 = \frac{\left(48B_0 + 48B_0h^2M\right)}{24Cr\,Dah - 10\beta Da}$$

$$C_6 = \frac{\left(B_0\chi h^2 + 48B_0Da^2M + 48B_0Da^2\right)}{2Cr\,DaB_0 + MDa}$$

The solvability requirement is determined by the boundary conditions and differential equations for temperature and concentration.

$$\int_0^1 W_1\, dz + \chi\int_{-h}^{0} W_{m1} dz = \frac{\left(1+\chi\right)\left(1+h\chi\right)}{\chi} \tag{38}$$

Back substituting the expressions for W_1 and W_{m1} into Eq. (38) and integrating the result yields an expression for the critical Marangoni number M_c, which is given by

$$M_c = \frac{24\left(12Da\,hB_0 + \delta_1\right)}{\left(\delta_2 + \delta_3\right)} \tag{39}$$

where

$$\delta_1 = \frac{\chi + 1}{24Da^2 - 10\chi\beta B_0}, \delta_2 = \left(\frac{48B_0h^2}{Da\ Cr} + \frac{20\beta Da}{h^3}\right) \quad ,$$

$$\delta_3 = \left(\frac{12B_0h^3}{Da\ Cr} + \frac{12Cr\,h}{B_0Da^3} + \frac{\beta CrDa^2}{Dah^3 + 1}\right)$$

6. Results and Discussion

The unique characteristic of self-rewetting fluid is the nonlinear dependence of its surface tension to temperature. Unlike fluid in normal convection, whose surface tension is supposed to be a monotonically linearly decreasing function of temperature in most cases, self-rewetting fluid could shift from one kind of behavior to another kind which is different as temperature varies. In the case when the surface tension of self-rewetting fluid decreases as temperature rises, surface tractions tend to encourage circulation.

Figure 2 shows how the permeability of the porous layer affects the start of thermocapillary convection when χ = 0.7, *Cr* = 0.001, β = 0.1 & B_0 = 0.1. It can be seen that if *Da* goes down, the critical Marangoni number goes up. This causes the start of Marangoni convection to be delayed. However, as the depth ratio *h* increases, long-wave mode emerges instability of the system. As the depth ratio *h* continues to increase, Surface tension soon loses its ability to maintain the stability of the system and long-wave instability gets intensified rapidly as *h* increases. It is noticed that the critical Marangoni number of long-wave mode is a monotonically decreasing function of depth ratio *h* of long-wave mode reaches its minimum at around 20.

The influence of crispation number on the M_c for various depth ratio h is plotted in Fig. 3 for fixed values of $\chi = 0.7$, *Da* = 0.0003, β = 0.1 & $B_0 = 0.1$. Fig. 3 illustrates that Crispation number *Cr* is a destabilizing factor as the marginal stability curves decrease as *Cr* increases. This effect is since a higher value, which indicates a reduced stiffness of the fluid layer's free upper surface, makes the configuration more unstable.

The variations in M_c as a function of thermal diffusivity ratio χ are shown in Figs. 4 for *Cr* = 0.001, $Da = 0.0003$, $\beta = 0.1$ & $B_0 = 0.1$ as a function of depth ratio. As can be seen from the diagram, increasing the value of χ lowers the critical Marangoni number, causing the system to become unstable. However, as the depth ratio *h* increases, the critical Marangoni number is increased to depth ratio *h* = 10, then it decreases rapidly as the further increase of h.

The effect of χ and β on the critical Marangoni numbers M_c is shown in Figure 5 as a function of *Da* for a fixed value of $Da = 0.0003, \beta = 0.1, Cr = 0.001$. It is observed that a decrease in *Da* and χ increase in the critical Marangoni numbers, and hence makes the system more stable. The effect of β, as seen from the figure, is insignificant for large values of χ.

The influence of depth ratio *h* on the configuration is demonstrated in Figs. 6 for various depth ratio *h*. As surface tension is a spurring factor, the velocity eigenfunctions for both the fluid (*W*) and porous (*W*) layers are shown in Fig. 6(a), 6(b), 6(c), and 6(d), in which the dashed line indicates the fluid-porous interface. It is observed that the convection is greater in the fluid layer, while the heat transfer in the porous layer is mainly due to conduction. Further, it is noted that the onset of convection occurs closer to the interface with an increase in the strength of downflow. However, the onset of convection appears to be shifted towards the top boundary as the strength of flow increases. And also noted that as depth ratio *h* increases, longwave mode emerges, which is stimulated by perturbation with a comparatively smaller wavenumber. Surface tension soon loses its ability to maintain the stability of the system and long-wave instability gets intensified rapidly as *h* increases.

The critical Marangoni numbers M_c obtained by employing the Beavers–Joseph [30] interface conditions for different values of *h* = ζ are presented in Table 1 for comparison. In the Table, the critical Marangoni numbers (M_c) obtained by the regular perturbation technique are given for ordinary fluids. We note that M_c values are in very good agreement with those obtained by the exact method.

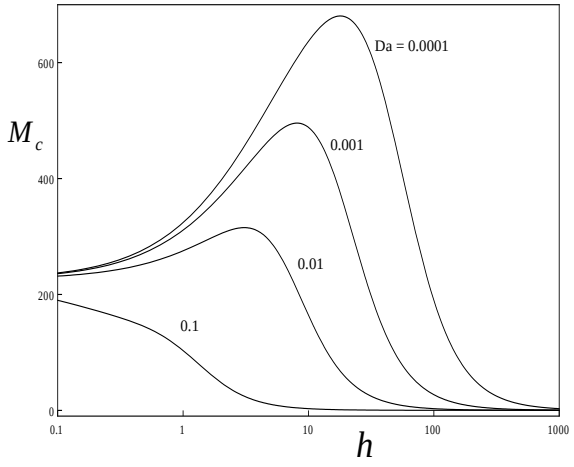

Fig. 2. Plot of M_c with h for distinct values of Da and fixed value of other parameters.

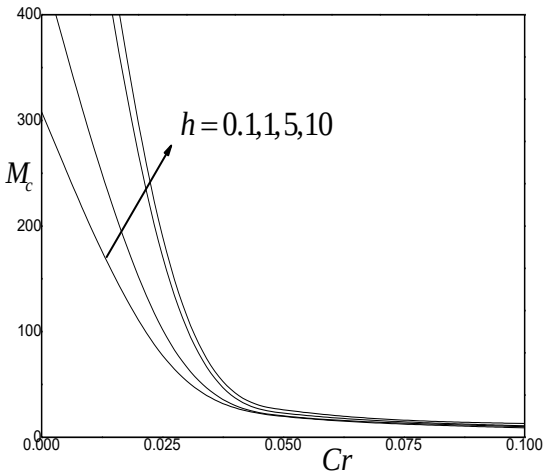

Fig. 3. Plot of M_c with Cr for distinct values of h and fixed value of other parameters.

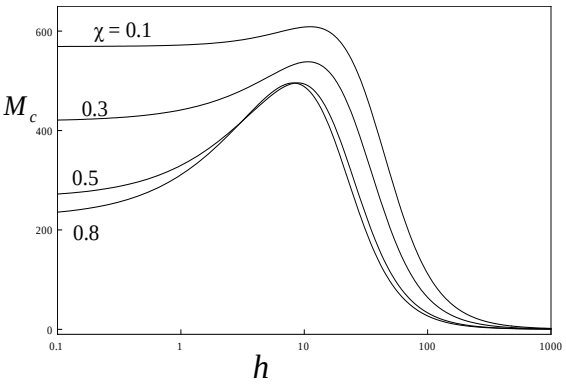

Fig. 4. Plot of M_c with h for distinct values of χ and fixed value of other parameters.

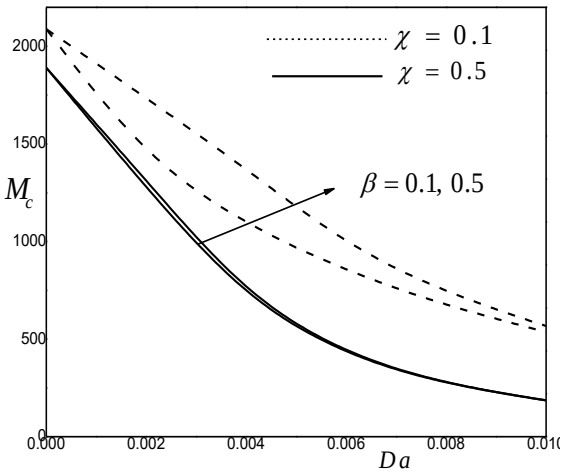

Fig. 5. Plot of M_c with Da for distinct values of χ and β for $h = 5$.

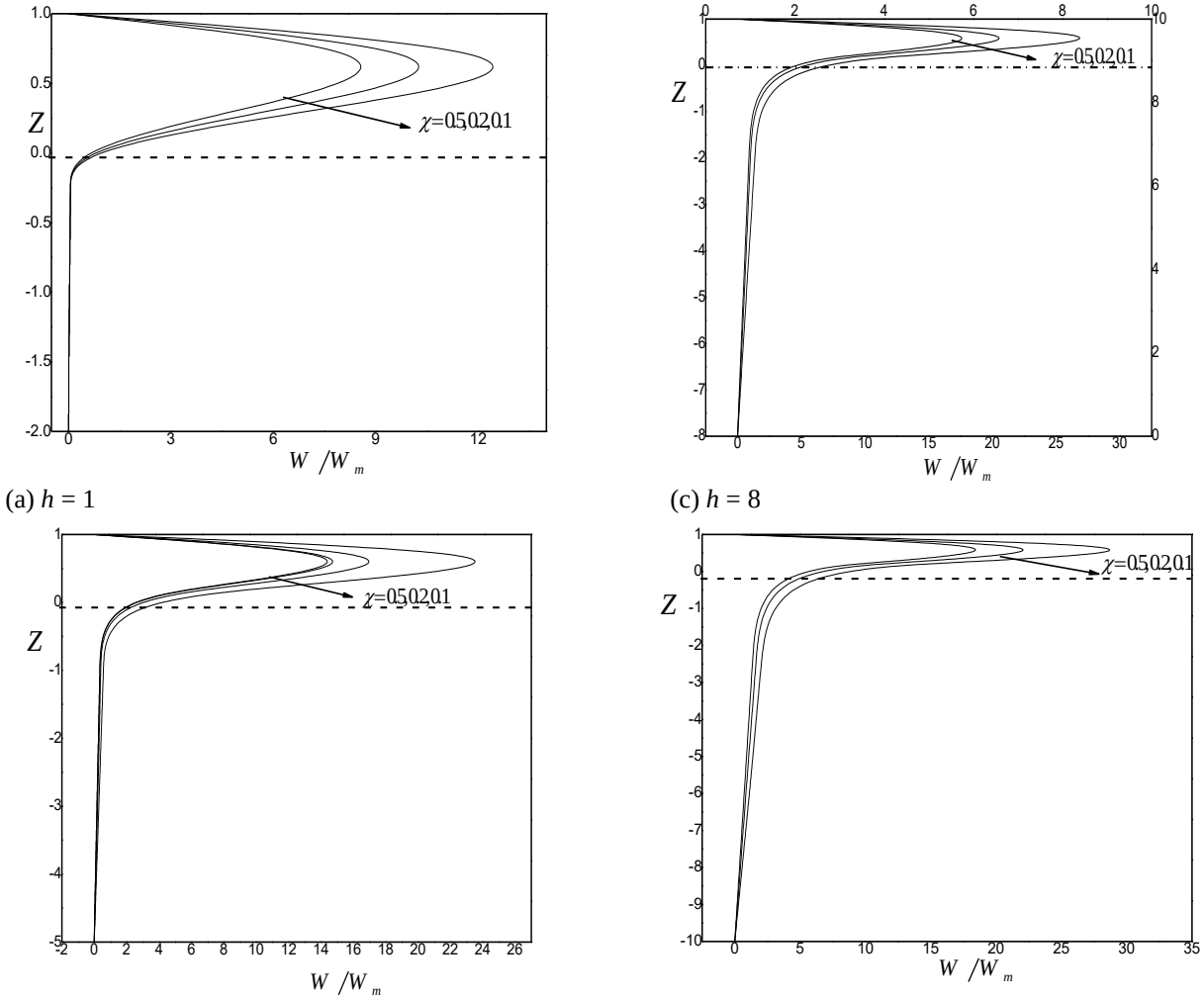

(a) h = 1 (c) h = 8

(b) h = 5 (d) h = 10

Fig. 6. perturbed vertical velocity versus eigenfunctions.

Table1. Comparison of critical Marangoni numbers for Beavers–Joseph (BJ) for ordinary fluids.

$h = \zeta$	M_c (BJ)	M_c (present study)
0.2	23.419	23.421
0.4	77.872	77.940
0.6	103.405	103.148
0.8	103.841	103.683

6. Conclusions

In this paper, we investigated the surface-driven convective motion in a self-rewetting fluid layer overlying a porous matrix subjected to a constant temperature gradient. The governing equation that satisfies the composite system is analyzed by the normal mode approach and solved by the regular perturbation technique for linear stability. Of interest are the influences of a quadratic relationship of surface-tension, depth ratio h, the Crispation number, the Darcy number, and the thermal diffusivity ratio χ on the onset of thermocapillary instability. The basic findings on how to control the onset of surface-driven convection in the bilayer fluid-porous medium are summarized below:

- With increasing Darcy number and thermal diffusivity ratio parameter, the size of convective cells decreases, however, depth ratio has a dual nature on the dimension of convective cells.
- Crispation number influences the onset of thermocapillary instability. The critical Marangoni number decreases as the Crispation number rises.
- An increase in the value of the thermal diffusivity ratio parameter decreases the critical Marangoni number, causing the system to become unstable.
- The depth ratio plays a crucial role in the control of the surface-driven convective motion in the bilayer system.

References

[1] Benard, H. Les tourbillons cellulaires dans une nappe liquid. Rev. Gn. Sci., Purea Appl. 11(1900)1261–1271.

[2] Pearson, J.R.A On convection cells induced by surface tension. Journal of Fluid Mechanics.4(1958)489–500.

[3] Nield, D.A. Surface tension and buoyancy effects in cellular convection. Journal of Fluid Mechanics.19(1964)341–352.

[4] Li, K., Tang, Z.M., Hu, W.R. Coupled thermocapillary convection on Marangoni convection in liquid layers with curved free surface. International Journal of Heat & Mass Transfer.55(2012) 2726–2729.

[5] Wu, Z.B., Hu, W.R. Thermocapillary migration of a planar droplet at moderate and large Marangoni numbers. Acta Mechanica. 223(2012) 609–626.

[6] Yin, Z., Gao, P., Hu, W., Chang, L. Thermocapillary migration of nondeformable drops. Physics of Fluids . 20(2008) 350.

[7] Shivakumara, I. S., S. P. Suma, R. Indira, and Y. H. Gangadharaiah. Effect of internal heat generation on the onset of Marangoni convection in a fluid layer overlying a layer of an anisotropic porous medium, Transp. Porous Med.92(2012)727-743.

[8] Gangadharaiah. Y.H. Onset of Benard–Marangoni convection in a composite layer with an anisotropic porous material, Journal of Applied Fluid Mechanics.9(2016) 1551-1558.

[9] Gangadharaiah YH and Ananda K, Influence of viscosity variation on surface driven convection in a composite layer with a boundary slab of finite thickness and finite thermal conductivity, JP Journal of Heat and Mass Transfer.19(2020)269-288.

[10] G.C. Rana, H.S. Jamwal. Hydromagnetic thermal instability of compressible Walters (Model B) rotating fluid permeated with suspended particles in porous medium, Studia Geotechnica et Mechanica. 35 (2013) 75 – 88.

[11] Gian C. Rana. The onset of thermal convection in couple-stress fluid in hydromagnetics saturating a porous medium, Bulletin of the polish academy of sciences technical sciences, 2014(62) 357-362.

[12] Gian C. Rana, R. C. Thakur, S. K. Kango. On the onset of double-diffusive convection in a layer of nanofluid under rotation saturating a porous medium , Journal of porous media.2014(17) 657-667.

[13] Rana, G., Chand, R. Stability analysis of double-diffusive convection of Rivlin-Ericksen elastico-viscous nanofluid saturating a porous medium: a revised model, Forsch Ingenieurwes. 2015(79)87–95.

*Corresponding e-mail: gangu.honnappa@gmail.com (Gangadharaiah Y H)

[14] Nield, D.A. Onset of convection in a fluid layer overlying a layer of a porous medium. Journal of Fluid Mechanics.81(1997)513–522.
[15] Chen, F., Chen, C.F. Onset of Finger Convection in a Horizontal Porous Layer Underlying a Fluid Layer. Journal of Heat Transfer.110(1998)403–409.
[16] Chen, F., Chen, C.F. Experimental investigation of convective stability in superposed fluid and porous layer when heated from below. Journal of Fluid Mechanics.207(1989)311–321.
[17] Beavers, G.S., Joseph, D.D. Boundary conditions at a naturally permeable wall. Journal of Fluid Mechanics.30(1967) 197–207.
[18] Zhao, S.C., Liu, Q.S., Liu, R., Nguyen-Thi, H., Billia, B. Thermal effects on Rayleigh-Marangoni Benard instability in a system of superposed fluid and porous layers. International Journal of Heat and Mass Transfer.53(2010) 2951–2954.
[19] Samanta, A. Role of slip on the linear stability of a liquid flow through a porous channel. Physics of Fluids.29(2017) 094103.
[20] Vochten, R., Petre, G. Study of the heat of reversible adsorption at the air-solution interface. ii. experimental determination of the heat of reversible adsorption of some alcohols. Journal of Colloid and Interface Science.42(1973) 320–327.
[21] ABE, Y. Self-rewetting fluids. Annals of the New York Academy of Sciences.1077(2016) 650–667.
[22] Straughan, B. Surface-tension-driven convection in a fluid overlying a porous layer. Journal of Computational Physics.170(2001)320–337.
[23] Gangadharaiah, Y. H., Suma, S. P. Bernard-Marangoni convection in a fluid layer overlying a layer of an anisotropic porous layer with a deformable free surface, Advanced Porous Materials.1(2013)229-238.
[24] Y. H. Gangadharaiah, K. Ananda, H. Nagarathnamma, H. Marangoni convection in superposed fluid and anisotropic porous layers with throughflow Malaya Journal of Matematik.8(2020)845-851.
[25] Gangadharaiah, Y. H, Double diffusive surface driven convection in a fluid-porous system, International Journal of Thermofluid Science and Technology, 8,(2021) 080301.
[26] Gangadharaiah, Y. H., Suma, S. P., Bernard-Marangoni convection in a fluid layer overlying a layer of an anisotropic porous layer with a deformable free surface, Advanced Porous Materials, 1(2), (2013)229-238.
[27] Gangadharaiah, Y. H., Influence of Throughflow Effects Combined with Internal Heating on the Onset of Convection in a Fluid Layer Overlying an Anisotropic Porous Layer, Journal of Advanced Mathematics and Applications,6 (2017)79-86.
[28] Gangadharaiah, Y. H., Effects of Internal Heat Generation and Variable Viscosity on Marangoni Convection in Superposed Fluid and Porous Layers, Journal of Advanced Mathematics and Applications,3 (2014)158-164.
[29] Vochten, R., Petre, G. Study of the heat of reversible adsorption at the air-solution interface. ii. experimental determination of the heat of reversible adsorption of some alcohols. Journal of Colloid and Interface Science.42(1973) 320–327.
[30] ABE, Y. Self-rewetting fluids. Annals of the New York Academy of Sciences.1077(2006)650–667.
[31] Cloot, A., Lebon, G. Marangoni convection induced by nonlinear temperature-dependent surface tension. J. Phys. France.47(1986) 23–29.
[32] G.S. Beavers, D.D. Joseph. Boundary conditions at a naturally permeable wall, J. Fluid Mech. 1967(30) 197–207.